Bi-Directional Bioelectronic Interfaces: System Design and Circuit Implications

1. INTRODUCTION

The total economic cost of neurological disorders exceeds £100B per annum in the UK alone, yet pharmaceutical companies continue to cut investment due to failed clinical studies and risk [1]. These challenges motivate an alternative to *solely* pharmacological treatments. The emerging field of "bioelectronics" suggests a novel alternative to pharmaceutical intervention, by using electronic hardware to directly stimulate the nervous system with physiologically-inspired electrical signals [2]. Given the processing capability of electronics and precise targeting of electrodes, the potential advantages of bioelectronics include specificity in time, method, and location of treatment, with the ability to iteratively refine and update therapy algorithms in software [3]. A primary disadvantage of current systems is invasiveness due to surgical implantation of the device.

This tutorial provides an overview of future bioelectronic systems using a control-theoretic approach. A bioelectronic technology stack for interfacing with the nervous system will provide the overall framework for the tutorial. We describe how the issues with the current generation of bioelectronic systems are being addressed with the new stack, and highlight areas of future innovation. To provide specific context for the platform, we will describe unmet clinical needs being explored currently in translational studies for Parkinson's disease, epilepsy, apnoea, and incontinence. The breadth of these examples reflects the diversity of challenges created by neurological disorders, but also the hope that bioelectronic systems can help address them.

2. OVERVIEW OF THE TECHNOLOGY STACK

2.1 The Bioelectronic Functional Block Diagram

A bi-directional bioelectronic system must support a complete closed-loop design from detection of physiological signals through updated actuation of the neural network. The key components of this flow are illustrated in Fig. 1, and take on the form of a neural co-processor [4]. The design intent of the neural co-processor is to create an adjunctive feedback loop in the nervous system, which can restore or replace functionality in diseased networks, and perhaps augment or enhance performance in the future (beyond the scope of this paper). To realize the co-processor concept [5, 6] we require: 1) a sensing interface to the nervous system or other input control variables; 2) a signal conditioning circuit that filters and digitizes the signals of interest; 3) a classification block that estimates the patient's physiological state based on sensed signals; 4) a control policy block that chooses the appropriate action to take based on classified state and desired outcomes including adjustment based on current goals; and 5) an actuator that applies stimulation to effect the neural state.

These functional blocks are mapped into discrete technologies. Key considerations include 1) the channel count for electrode interfacing for sensing and stimulation, 2) the amplifier bandwidth and noise floor to align to the signals of interest, and 3) the strategy for signal processing – either hardware subroutines in analog or digital signal processing or use of a programmable processor. In parallel with this signal pathway, we must also consider infrastructure for databases, models and methods, such as machine learning for reinforcement of the desired behaviour, material interfaces and packaging, as well as telemetry. Note that this signal pathway is not limited to the central nervous system, and can be broadly used in the periphery in applications such as cardiac pacing [7], spinal cord stimulation [8], or sleep apnoea therapy [9]. The next sections provide more systematic reviews of each area, with an emphasis on the circuit requirements for the neural interface.

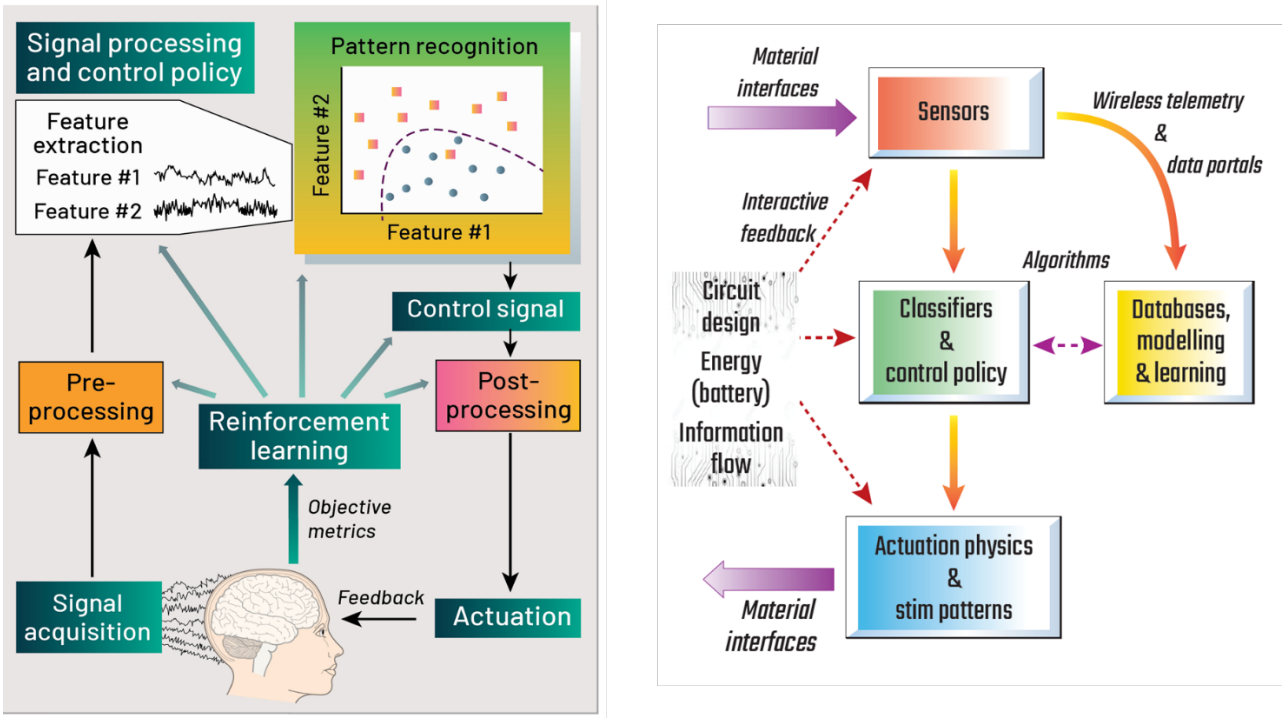


***Figure 1**. Left: The functional flow design of bioelectronic systems and Right: the supporting technology stack.*

3. NEURAL SENSING

Future and emerging applications that require neural recording capability are driving trends in the development of integrated systems for next-generation neural interfaces. These are demanding more channels, higher integration densities, and the ability to maintain recording integrity during stimulation. The key current applications in development are research tools for neuroscience, brain-machine interfaces and closed-loop neuromodulation devices [10-12]. In this section we outline the trends and explore the implications these pose to the integrated architecture and circuit implementation.

3.1 System Organisation

As neural recording systems increase in complexity, we are seeing changes to the overall system organization deviating from the traditional modular approach. Systems are now optimizing a hierarchical organization to cater for increasing numbers of channels, with varying granularity in the circuit architecture, and system partitioning across multiple devices. Neural interfaces (i.e. electrodes) are also being monolithically integrated.

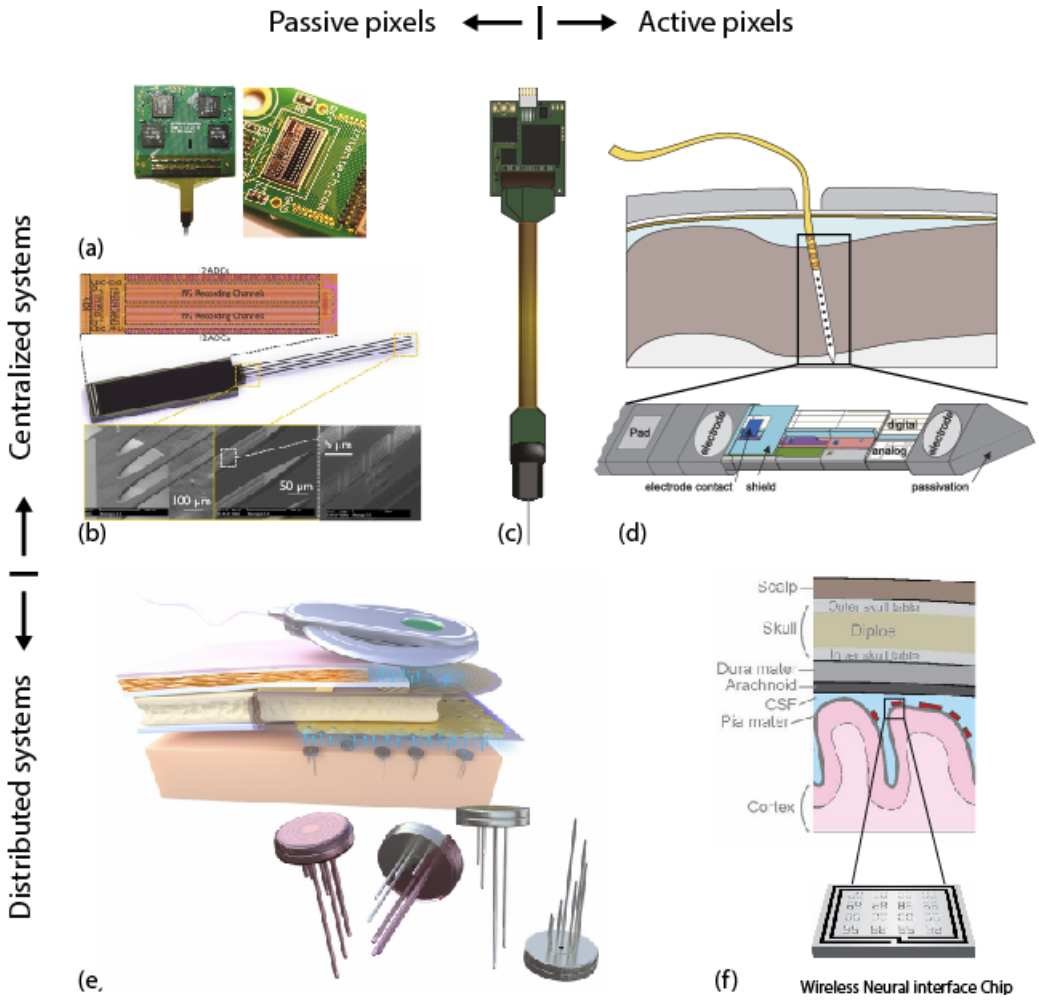


Figure 2: *Examples of different implantable recording system organizations: (a) Intan system integration [3]; (b,c) neuropixels [2] and; (d) IMTEK active probes; (e) ENGINI [5]; and (f) ENIAC distributed system [4].*

3.2 Centralized vs. Distributed Systems

With modern integrated circuit and microsystem technologies, multi-channel neural recording systems can easily be implemented on a single chip to combine signal conditioning with data conversion, processing and communication capability. Key examples include neuropixels probes [13] and the Intan electrophysiology IC [11].

This centralized, single-chip approach mitigates the system integration effort by exploiting commercially available CMOS technology. Also, by multiple channels sharing circuits such as data converters, digital filters and data-transmission drivers, physical resources can be minimized. However, as centralized systems are further up-scaled in channel count (e.g. towards and beyond 1,000 channels), the overall power consumption poses a challenge in maintaining safe levels of thermal dissipation for neural tissue. Wire routing also becomes a challenge, so such systems are constrained to high-density probes with integrated electrodes.

However, for applications that require observing neural activity across a larger region of tissue, splitting the system into several, smaller probes presents a relatively new distributed approach. Here, each sub-system must integrate the neural recording function (and also possibly stimulation capability) with wireless power management and data communication, and ideally should operate autonomously. This architecture, therefore, shifts the challenge to achieving means of efficient wireless power and data transfer. Key examples include ENIAC/neurograins [12], ENGINI [14], and neural dust [15] (Figure 2).

3.3 Passive Electrodes vs. Active Probes

Systems that use conventional (passive) neural probes, electrodes (e.g. microwires) and microelectrode arrays are modular and not fully integrated. They, therefore, require external wiring for connection to integrated recording systems, typically using multi-conductor cables with connectors, and/or wirebonding/flip-chip bonding. The number of conductors then scales linearly with the number of electrodes, resulting in significant engineering challenges in the assembly and mechanical reliability of high channel count systems.

Fully integrated systems (i.e. active probes) leverage on microsystems technology allowing for the monolithic integration of electrodes and electronics through 'circuit under pad' design [13]. This can allow for multiplexing, amplification, or even data conversion beneath the electrode, and brings the benefit of minimising crosstalk and/or the sensitivity to biological or environmental noise. This, however, comes at a cost: the added design challenge to minimize the power and area of the front-end, given that the electrode pitch is limited by the spatial resolution requirement for neural signal recording. Furthermore, the electrodes themselves need to be fabricated using materials and a process flow that are CMOS compatible.

3.4 Instrumentation Architecture

Within the integrated electronics itself, instrumentation systems have been extending their functionality from originally just signal amplification, to subsequent conditioning, data conversion and signal processing. This trend is illustrated in Figure 3. With this increasing integration complexity, front-end amplifiers that previously had parallel or multiplexed analog outputs are now being converted on chip, to output digitally-sampled or compressed data streams. This allows for high bandwidth, data communication that is robust to environmental noise. With technology scaling, power savings in previously multiplexed analog or raw digital streaming allows for digitization and post-processing within the same power/area envelope. Furthermore, in-channel integration of the analog front-end and data conversion avoids needing analog multiplexing and the requirement for signal settling in data-converter sample-and-hold circuits.

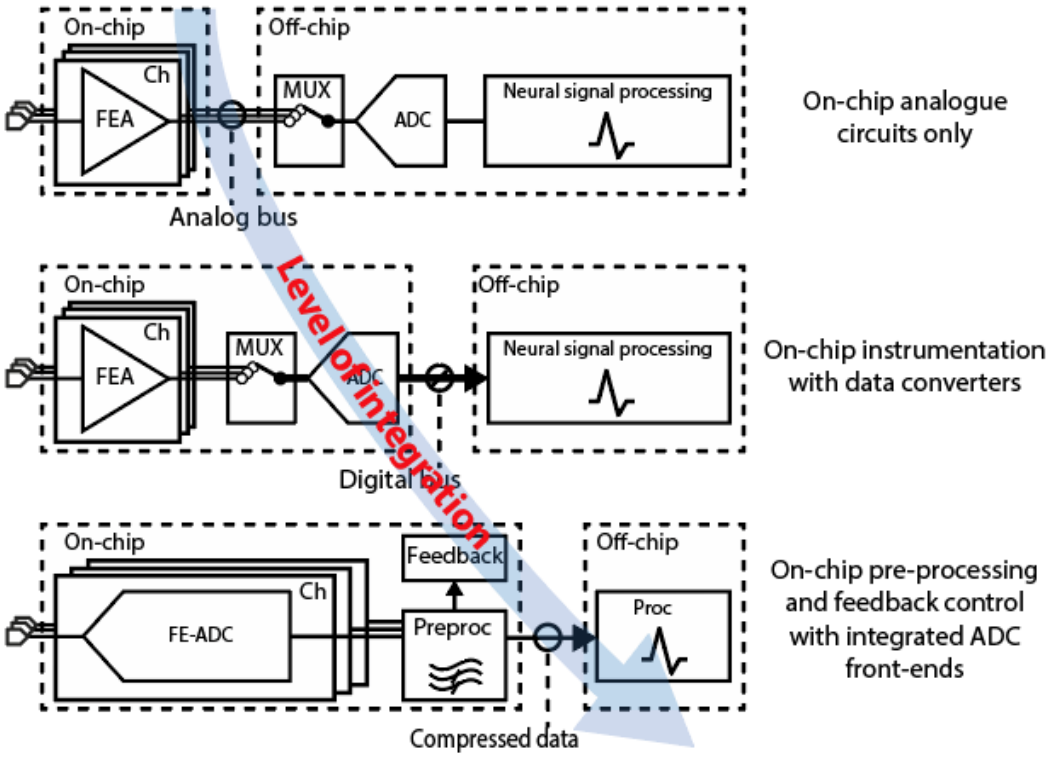


Figure 3: *Trends in the integration of neural recording systems.*

3.5 Front-end Circuit Implementation

Whilst digital processing circuits benefit greatly from technology scaling, the front-end mixed-signal design still requires significant design effort to achieve the required performance (noise, bandwidth) for minimum resource (power, area). The circuit topology here plays a key role in the overall system design to achieve a better FOM.

3.5.1 Key Requirements

The main technical requirements for a neural recording system are given in Table 1. In a typical neural recording system, the differential signal observed between a recording and reference electrode is amplified, filtered and digitized. This needs to remove the DC offset (due to the electrode-tissue interface) and reject common-mode signals to avoid saturation and/or distortion in the front-end amplifier. This can also be mitigated by implementing a front-end with high dynamic range (DR), also relaxing requirements of a low-frequency cut-off and high CMRR. A high DR front-end can allow for DC-coupled or single-ended inputs, if the recording and reference inputs are acquired separately and the difference calculated in the digital domain. This can also be of benefit to bidirectional neural interfaces, where stimulation patterns can manifest themselves as large artefacts of up to several hundred mV and potentially saturate analog front-ends.

Table 0. *Key technical requirements for neural recording systems*

Specification		Typical	Comment
Recording Performance	Noise (µVrms)	<5	Including both electrode & instrumentation noise
	Bandwidth (Hz)	1-3000	Broadband to include local-field-potential (LFP) and extracullar action potential (EAP) signals
	DC rejection (mV)	>100	Offset across different electrodes
	Dynamic range (dB)	>50	Relating to front-end amplifier, data converter
	CMRR (dB)	>70	For interference/stimulation artefact suppression
	PSRR (dB)	>70	Voltage regulation can relax this requirement
	Input impedance (Ω)	>5M	Large compared to electrode impedance
Resource per channel	Area (mm^2)	0.01-0.1	To allow for large channel counts
	Power (µW)	10	Limited by heat dissipation in tissue

3.5.2 Circuit Topologies

Over the past 3 decades, we have witnessed significant progress in the design of integrated circuits for neural recording. In particular, the noise efficiency factor (NEF), a FOM quantifying how much current is required to achieve low noise, has been massively improved. This is illustrated in Figure 4.

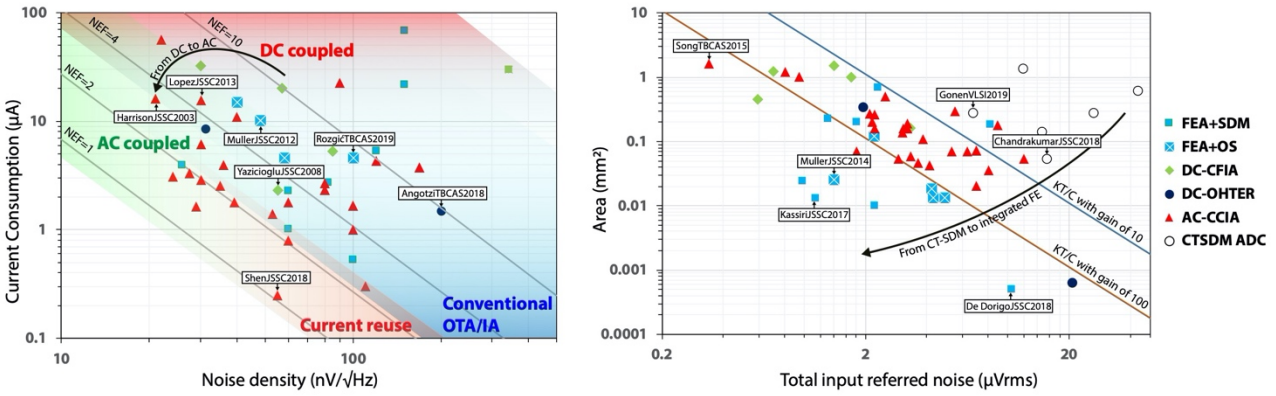


Figure 4: *Performance comparison of analog front-ends for neural recording, showing: (a) noise spectral density versus current consumption; (b) total noise versus silicon area.*

Current-feedback instrumentation amplifiers (CFIA) offer excellent CMRR, however, have added noise contribution from the resistors and require active feedback to remove low-frequency components (i.e. electrode offset). AC-coupled amplifiers (CCIA) simplify low-frequency rejection

by using either a pseudo-resistor (PR) network or capacitive feedback (with the PR to establish the DC level). This greatly improves the NEF from 6 to 4 [11], and current-reuse or stacked transconductors further push the NEF towards the theoretical limit. While the NEF has been greatly improved with a reduced noise spectrum density, the total in-band noise remains correlated to the area, which can be estimated by the KT/C thermal noise [11] and gain, shown in Figure (b). Although implemented in different circuit architectures, the noise and area of the 1st stage amplifiers are dominant in CCIA and CFIA configurations. Therefore the majority of designs in the literature fall into the rough estimation boundary between a gain of 10 and 100, with a capacitance density of 1fF/μm^2. It should be noted that several designs that have been included in Figure (a) combine the front-end amplifier with the data converter, thus quoting a combined power. Such configurations thus could reduce power consumption and area.

With an oversampling (OS) ADC or integrated IA with a sigma-delta modulator (SDM), the in-band noise can be shaped by the noise transfer function and oversampling ratio, without aliasing broadband noise into the signal band. Therefore the constraint between area and in-band noise is relaxed, as shown in Figure (b). With these integrated IA+SDMs, the feedback path can realize both low-frequency rejection and modulation, therefore further reducing the total area, attenuating in-band thermal quantization noise level for a high DR. It is also interesting to see CT-SDM ADC designs from the data-converter community are approaching the range of neural front-ends [15]. With joint effort in both domains, further optimisation is possible to achieve highly integrated solutions with large artefact tolerance.

4 Neural Signal Processing: Classifiers and Control

Current and emerging applications require processing of neural recordings in real time: brain-machine interfaces require neural decoding of intention [10], whereas closed-loop neuromodulation requires feature extraction and biomarker identification. A typical neural signal-processing flow, for the two key types of neural signals observed in implantable devices, viz. local field potentials (LFP) and extracellular action potentials (EAP), is shown in Figure 5. Both signal types follow a similar processing flow (feature enhancement/extraction, dimensionality reduction, classification, feedback) [16], but using different features and analysis methods.

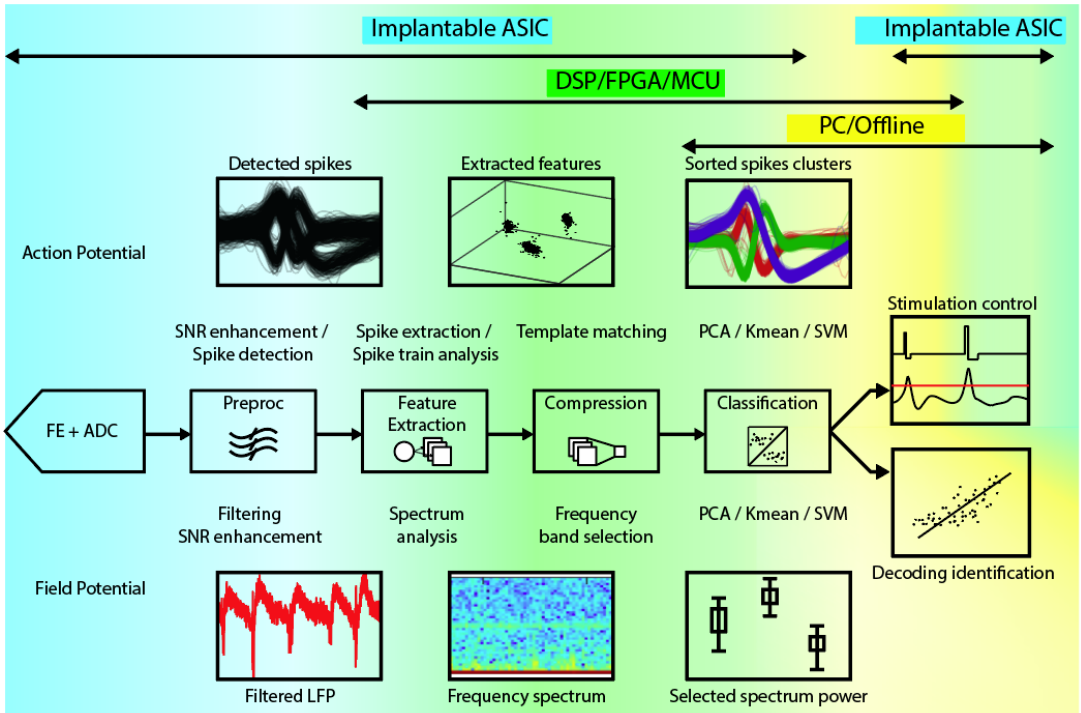


Figure 5: *Neural signal processing for real-time, closed-loop applications.*

4.1 Processing Methods

Typical examples of methods for neural signal processing are listed in Table 4-1. Both signal types share analysis methods, such as filtering and principal-component analysis (PCA). EAP processing tends to utilize more time-domain analysis methods such as spike detection, sorting, train analysis, whereas LFP processing tends to focus more on frequency content. For bidirectional design, feedback parameters are calculated and evaluated based on a control policy that is patient-specific.

Table 4-1: *Typical neural processing methods*

Processing steps	**LFP (Low frequency)**	**AP (High frequency)**
Preprocessing	Filtering, energy operator	Filtering, spike detection, validation
Feature extraction, dimensionality reduction	Power spectrum at certain bands, time-domain power and amplitude, PCA, thresholding	Spike snippet, derivatives features, time interval between spikes, PCA, wavelet analysis, thresholding
Classification, decoding	*k*-means, template matching, support vector machine (SVM)	
Feedback control	Neural networks, phase locking, proportional-integral-derivative (PID) control, model predictive control (MPC), rule-based, thresholding	

4.2 Hardware Implementation

Considering how tight the power and area requirements are for neural recording systems, conventional schemes for neural signal processing are relatively computationally and memory intensive. It is thus essential to partition the processing flow between on-chip (e.g. ASIC), off-chip/on-node (e.g. FPGA, DSP), and off-node (computer, cloud). A typical workflow would operate hard-coded feature extraction options on-chip, thus also reducing data bandwidth for off-chip wireless or wired communication. Subsequent real-time processing (classification and/or inference) would be performed on-node on an embedded and/or reconfigurable hardware platform. This would allow for closed-loop feedback in a low-power standalone, autonomous system, for example, active implantable medical device, typically integrated at board level. Offline analysis including training and/or calibration would be performed off-node on a workstation or cloud service.

5 Neural Stimulation

Electrical stimulation has been the traditional method to interact with the nervous system. Integrated circuits have been an enabling technology for the developments in this field, and today it is possible to have hundreds and thousands of stimulating channels in a single chip [17, 18]. With the demand for higher spatial resolution and with the resultant need for *safety* and *higher power efficiency*, there are several challenges in which new circuits and architectures can play a vital role. In parallel, the fields of optogenetic and ultrasound neuromodulation have emerged as alternatives to electrical stimulation, both providing different and attractive properties. The trend in these fields has been to move from bulky laboratory setups into integrated and miniaturized systems, in which high density and safety considerations must also be guaranteed. Here, we discuss the electrical, optogenetic and ultrasound stimulation modalities and the role of integrated circuit design as an enabling technology for further advancement of the field of neuronal stimulation.

5.1 Electrical Stimulation Methods

The goal of electrical stimulation for activation of excitable cells, such as cardiac, muscle and neuronal cells, is to deliver a well-defined amount of *charge* (or rather, *charge density*, in $\mu C/cm^2$) to the tissue to build up a specific electric field distribution in the tissue such that an action potential is generated (anodic phase), and subsequently remove the charge (cathodic phase). This stimulation sequence is called a biphasic pulse. It should be noted that high-frequency (> 1 kHz) stimulation can also block action-potential propagation. Though electrical stimulation can be accomplished by means of voltage, current and charge [17, 19, 20], most stimulators use current sources to build up and remove the charge from the tissue. A generic biphasic, constant-current, stimulation setup is shown in Figure 6. Generally, two electrodes (el_1, el_2) are required for (bipolar) stimulation, although multi-

polar stimulation by means of multiple electrodes is sometimes also used to generate a specific electric field pattern in the tissue.

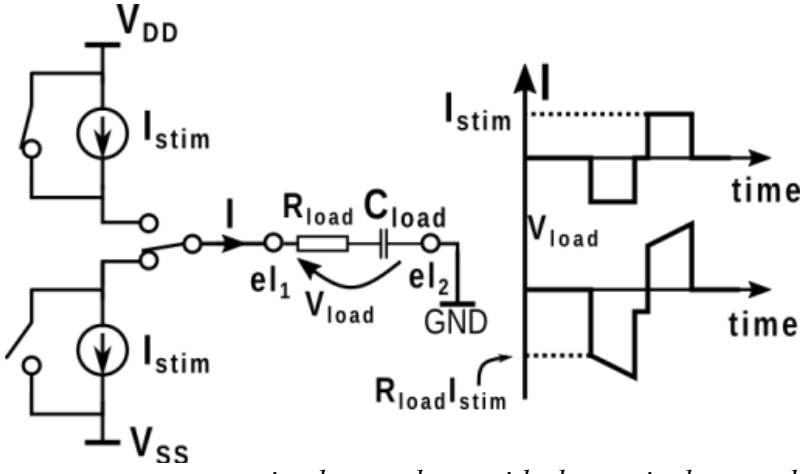


***Figure 6**: Biphasic-constant current stimulator, along with the equivalent model of the electrode-tissue interface and the stimulation current and resulting voltage across the electrode-tissue interface.*

The electrode-tissue interface, to a first approximation, can be modeled as a resistance R_{load} with a series capacitor C_{load}. During stimulation, there is a constant voltage drop $R_{load}I_{stim}$ across R_{load}, while capacitor C_{load} is being charged with a constant current I_{stim}, leading to an affinely increasing voltage V_{load} across the electrode-tissue interface.

An important safety aspect for all neural stimulators is the excess of charge at the electrode-tissue interface of neural stimulators. At the end of a biphasic pulse, there will still be residual charge at the electrode-tissue interface, e.g. due to device or circuit mismatch, but most often as a result of the inherent non-linearity of the tissue itself. This residual charge must be avoided as it leads to electrolysis and thereby to tissue damage. To this end, typically a medical-grade, external capacitor is placed between the output of the stimulator and the electrodes such that it prevents any DC current to reach the electrode-tissue interface. However, it has been proven that this coupling capacitor introduces an offset voltage over the electrode-tissue interface, which depends on the electrode type and the intensity of the stimulation [21]. This offset voltage should not exceed the safety boundaries as this leads to irreversible electrochemical reactions. Moreover, medical-grade DC-blocking capacitors, being bulky external components, significantly contribute to the overall size of the implant and reduce the reliability of the whole stimulator. An alternative and safer approach to reach charge balance is to briefly monitor, and eventually actively correct, the electrode voltage after each biphasic pulse, either by means of a pulse-insertion technique [22] or by means of adjusting the duty-cycle of the biphasic stimulation pulse [23].

Another significant challenge that today's neural stimulators have in common is their limited battery life. Most primary cell batteries for neurostimulators last three to five years, and, in case of extensive use, the battery has to be replaced more often or a rechargeable system is used [24]. Furthermore, in the emerging field of Bioelectronic Medicine, to directly interface with tiny nerves, neural implants need to be made so small that a battery-less solution might be necessary, for which all available power would have to be harvested in or transferred from outside the body [25]. Hence, the need for increased power efficiency is more relevant than ever. At the same time, there is a need for an increasing number of independent stimulating channels to accommodate a large number of stimulating sites to achieve a larger spatial resolution. In applications like retinal implants several hundred or even a thousand stimulation channels are implemented [18]. Due to the high number of stimulating channels, the overall size of the stimulator increases at the expense of its safety (post-surgery trauma, risk of infection, charge accumulation). These three requirements, namely power efficiency, multichannel operation and safety, are not trivial to accomplish simultaneously. In the rest of this subsection, we

will look at the combination of power efficiency and safety of high-density multichannel neural stimulators.

To be able to drive every electrode with the right amount of charge (density), each electrode needs to be driven independently. The driver circuits of these electrodes, traditionally, are operated from a single high-voltage supply [17, 18], degrading the overall power efficiency as not all electrodes develop the same voltage and, as a consequence, a lot of voltage headroom is being wasted. The best power efficiency of multi-channel stimulator circuits, therefore, can be achieved by not driving every electrode from its own (current or voltage) driver circuit, but by using an Ultra High-Frequency (UHF) pulse-based technique that builds up the right amount of charge at every electrode by means of rapid (e.g., 1 micro-second duration) current pulses [19].

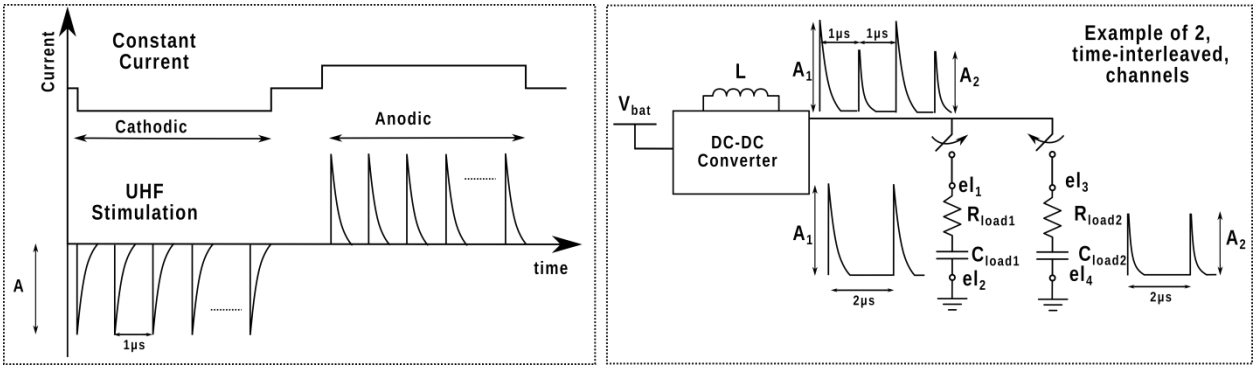


Figure 7: *(left) Sketch of a biphasic pulse produced by a constant current stimulator [12] (top) and by UHF stimulation (bottom); (right) high-level architecture of a UHF neural stimulator with its current waveforms during multichannel operation.*

In such a UHF pulse-based current-stimulator circuit, each stimulation phase is made of a sequence of current pulses injected into the tissue at a high rate. The amplitude of the pulses, indicated as A in Figure 7 (left), can be regulated and sets the stimulation intensity. A buck-boost DC-DC converter without the output filtering capacitance is used to generate the pulses. When more channels are operated concurrently, the pulses generated by the only inductor are sent to all the activated channels in a time-interleaved fashion. See Figure 7 (right). This technique avoids the use of a high-voltage supply, thereby maximizing the power efficiency while allowing the architecture to be scaled up to potentially several hundreds of electrodes. Moreover, the use of a buck-boost converter topology renders the stimulator circuit single-fault tolerant and thus no longer necessitates the use of (bulky medical-grade) coupling capacitors.

5.2 Optical Stimulation Methods

Alternative methods for actuating the nervous system are becoming available; we highlight two in this tutorial. The first is *optogenetic stimulation*, which is a cell-type-specific stimulation method that combines photonics and molecular genetics [26]. This method allows for the excitation and inhibition of neural networks in deep brain structures at very high spatio-temporal resolution. Optogenetic neurostimulation fundamentally relies on emitting light at a specific wavelength and intensity to electrically activate or inhibit genetically modified light-gated ion channel proteins in the neurons, the so-called ‘opsins’. There are many families of opsins but, typically, Channelrhodorpsin-2 is the opsin used for activation of the neural cells when exposed to a band of blue light (440 - 500 nm) and an intensity threshold below 1 mW/mm^2, whereas Halorhodopsin inhibits the neural activity when exposed to a band of yellow light (540-600 nm). A more detailed review on how optogenetics can be used for neural interaction can be found here [27].

Light can be delivered to the neural tissue by using custom-engineered devices combining light emission and electrical recording, the so-called *optrodes*. The construction of precise, smart and seamlessly integrated optrodes is an engineering challenge that involves multidisciplinary endeavors. Photolithography is the method of choice for fabricating optrodes because of its reproducibility, easiness of patterning precise structures with high-aspect-ratio resolution, and CMOS compatibility. However, true seamless integration of light sources on the optrode still remains one of the most difficult challenges. This is mainly caused by the intrinsic need of using substrates where direct bandgap materials (e.g., GaN or GaAs) can be grown with minimum lattice mismatch so as to provide high-efficiency light emission at a specific wavelength. Currently, mainly two approaches to deliver light as close as possible to the target at sufficient intensity for effective optical stimulation have been used: *integrated optical waveguides* and *in-situ LED probes*.

5.2.1 Integrated Optical Waveguides

In the first approach, light is delivered to the target by an external unpackaged photonic device coupled to a planar optical waveguide integrated on the probe and engineered by standard photolithographic techniques. However, the coupling between the photonic element and the optical waveguide usually creates significant insertion losses (often in the range from 90 – 95%) due to intrinsic and extrinsic properties [28] such as misalignment. This hinders the necessary light intensity to be delivered at the target tissue.

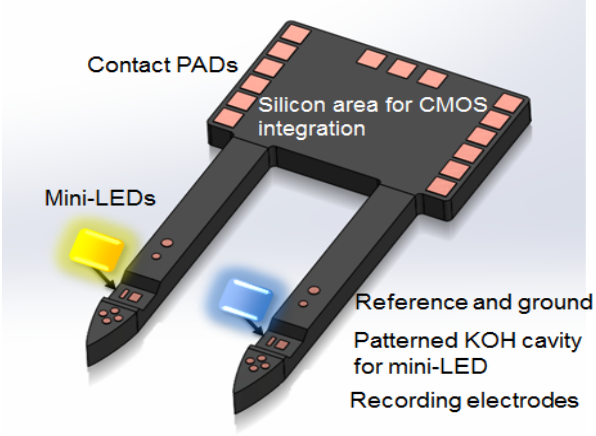


***Figure 8**: Artistic impression of a micromachined silicon-based optrode for heterogeneous integration of mini-LEDs.*

5.2.2 In-Situ LED Optrodes

A possibility to circumvent the optical losses of the previous method is bringing the photonic source itself as close as possible to the brain tissue by means of heterogeneous integration. Hence, the light intensity can be maximized and well controlled at the brain-region target. This method offers a good trade-off between radiant intensity and the possibility of integrating high-density CMOS functionality on the same probe. The probe can be constructed and customized using MEMS-based photolithography methods. The optrode of Figure 8, for instance, was customized to allow for experimentation of activation and inhibition at different locations of the brain, simultaneously. To reduce the topography produced by the thickness of the mini-LEDs, cavities can be anisotropically etched using a tetramethylammonium hydroxide (TMAH) or potassium hydroxide (KOH) solution. The recording electrodes can be patterned with non-standard CMOS materials, such as Titanium Nitride or Poly(3,4-ethylenedioxythiophene) (PEDOT), to reduce the electrode-tissue interface impedance. Commercial mini-LEDs with reasonable (up to 30%) power efficiency can be flip-chip bonded. The light intensity of the mini-LEDs can be controlled by a PWM control circuit. The challenges of this heterogeneous approach include ensuring proper isolation of the electrical contacts to prevent uncontrollable current leakages to the tissue, as well as avoiding early corrosion of the contacts due to moisture and the associated redox reactions.

5.2.3 Final Considerations for Optogenetic Stimulation and Relevant Translational Challenges

In spite of the recent advances in the photonics field to yield efficient devices with different functionalities, such as photoemission, transmission, and detection, seamless integration of photonic

sources for minimally-invasive procedures in optogenetics is still a claim under dispute. Two different methodologies are currently being investigated among different research groups: waveguiding and in-situ photonic sources. In the first one, MEMS-based photolithography technology offers a way to construct precise and reproducible engineered structures for bridging the gap among the dissimilar photonic components required in the neural probe. However, constructing efficient light couplers is still a critical point to render sufficient light intensity to the target. The second approach refers to the heterogenous integration of commercial LEDs on a scalable CMOS neural probe. MEMS technology offers the possibility of anisotropically etching structures for integrating the light sources and defining precise silhouettes for minimally invasive procedures. Preventing uncontrollable electrical or thermal stimulation stemming from the LEDs, while providing sufficient light transparency, protecting the device against moisture ingress and ensuring the necessary biocompatibility are crucial features to be addressed by advanced packaging strategies. For a more detailed review regarding available technologies for optrodes and the associated heat generation, coupling and packaging challenges the reader is refered to [28].

Aside from the aforementioned technical considerations, bringing optogenetic tools to human therapy poses its own unique challenges. More specifically, rendering the cells sensitive to light, which for research purposes is done via gene modification, for use in humans requires a complex process for regulatory approval [29]. To this end, transplanting already modified cells could instead be a more viable alternative. Furthermore, current animal studies have not been conducted over a long enough time, so any potential adverse effects are not yet fully understood [30]. Last but not least, risks related to how bacteria-originated optogenetic tools will be accepted by the human cells have to be mitigated.

5.3 Ultrasound Stimulation Methods

Currently emerging as a new modality for stimulating neuronal circuits in the brain is the field of *focused ultrasound stimulation* [31, 32]. Traditionally used in diagnostic medical imaging, the propagation of ultrasound energy in soft tissue provides very different and attractive properties for usage as a neurotechnology modality when compared with electrophysiology or optogenetics: it can be applied non-invasively at the surface of the skull (for brain) or skin (for peripheral nerves), or minimally invasively on top of the dura mater. Ultrasound can penetrate several centimeters in the brain, and can be focused in specific locations with high precision and sub-millimeter to millimeter spatial resolution.

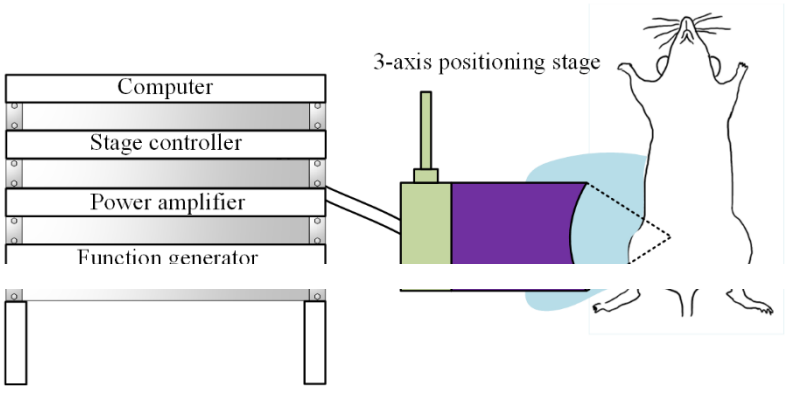


***Figure 9**: Typical setup for peripheral nerve stimulation with focused ultrasound*

An example of a traditional experimental setup for ultrasound neuromodulation, in this case of peripheral nerves, is illustrated in Figure 9, and consists of using a focused ultrasound transducer, typically implemented by a piezoelectric material such as Lead Zirconate Titanate (PZT). It is coupled into tissue using a coupling gel to avoid air, and is driven by a function generator and a power amplifier. The geometrical focal depth of the ultrasound wave depends on the radius of curvature of the transducer, and for that reason it is typically connected to a 3-axial stage for adjusting the stimulation location.

The goal of current research efforts focuses on understanding how the sonication parameters influence the resulting neuronal activity. Stimulation typically involves bursts of focused ultrasound

waves with durations from tens of µs to a few ms, with pulse-repetition frequencies from 1 Hz to a few kHz, and focal pressures from a few hundreds of kPa to a few MPa. It has been shown that longer burst durations with lower pressures lead to inhibition of neuronal activity and shorter burst durations with higher pressures lead to activation, and that higher pressures are required to stimulate peripheral nerves compared to those required for stimulation of the brain [33, 34]. Besides understanding the effect of the different stimulation parameters on neuronal activity, it is of paramount importance to understand if there is indeed a set of parameters that succeed in either activating or inhibiting a target neuronal circuit without leading to damage of the tissue. The FDA imposes a limit for the spatial peak temporal average intensity (I_{SPTA}) for ultrasound medical imaging of 720 mW/cm^2, which can be an obstacle, specifically for the peripheral nerves that seem to require higher focal pressures [34]. Assuming parameters for safe interaction with neurons can be achieved, the bottleneck will rapidly become the large form factors of the ultrasound transducers and interfacing electronics, the limited targeting ability of the focused transducer [35], and how to add a non-invasive or minimally-invasive neuronal recording modality with similar properties to the system, to allow for closed-loop stimulation. For the reasons above, system integration of electronics and transducers can play a vital role in the future of this field. By exploring high-efficiency phased-array transmit beamforming circuits [36, 37] with architectures tailored for the specificity of ultrasound neuromodulation, such as longer pulse durations and higher focal pressures, miniaturized ultrasound stimulators with high spatial resolution and electronic controlled focal spot location can potentially be achieved.

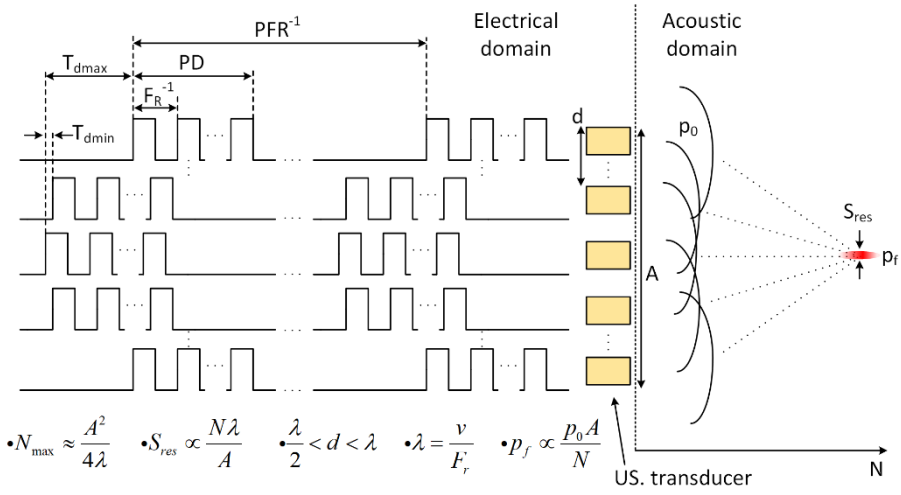


Figure 10: *Variable space in ultrasound phased arrays*

In Figure 10, the relation between the relevant properties of acoustic waves and the required parameters of the ultrasound transducer array driving signals is shown. Since each driving circuit must be directly below the corresponding transducer to allow for pixel-pitch matched beamforming, a tradeoff has to be made between performance (spatial resolution (S_{res}) and focal pressure (P_f)) and available power/channel and circuit area/channel. Hence, circuit architectures that can tackle this tradeoff are required, with potential strategies illustrated in Fig. 11. Moving the beamforming circuitry between the periphery (blue) and the array channels (yellow) results in different circuit and routing (purple) complexities. For small arrays and high-frequency operation, strategy A might be a good choice due to the small available area in each array channel, at the expense of higher routing complexity (one signal per channel). With large arrays with low frequency of operation, strategy B is a viable option, due to the larger available area per channel and lower routing complexity (only one clock), however, the available power/channel will be lower, thus requiring high power efficiency. When high channel count and high frequency is needed, strategy C might be the best option, with the beamforming complexity shared between the periphery and the channel circuitry, and with medium routing complexity.

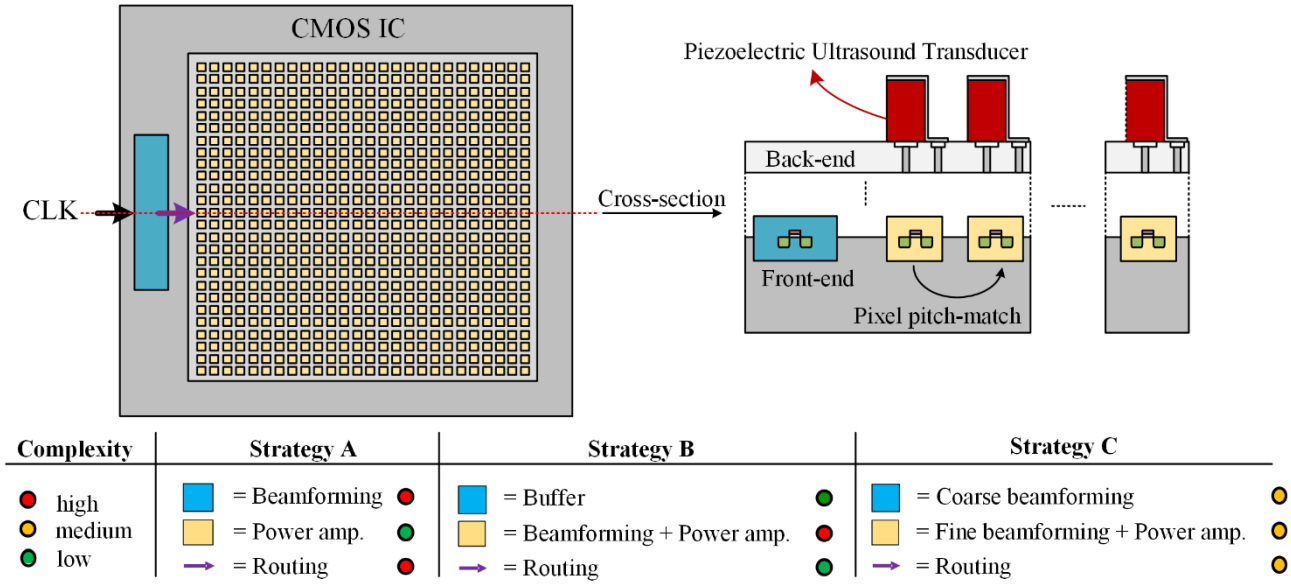


Figure 11 *– Different strategies for implementing phased-array transmit beamforming circuits tailored for ultrasound neuromodulation*

Researchers have developed a first attempt in miniaturizing an ultrasonic neuromodulation device based on phased arrays [38], however, the achieved focal pressure (100 kPa) is still lower than required. To improve this, optimizations in the transducer microfabrication, such as the inclusion of an acoustic matching layer, and also the use of high-voltage CMOS technologies, might be able to bring the focal pressures into the MPa range. Furthermore, increasing the focal depth while maintaining or even improving the spatial resolution will require larger transducer arrays, leading to the need to develop more power-efficient beamforming circuits. To allow for both neuronal stimulation and either ultrasound structural [36] or functional imaging [39], analog front-ends, receive beamformers and other signal-processing circuitry can be added to systems of this nature, which can potentially pave the way for non-invasive or minimally-invasive closed-loop interfaces to the nervous system.

6 Additional System Considerations

Although we are limited in space, it is important to highlight a few other key areas of system integration that are required for a complete system as they relate to circuit design. Specifically here, in order to achieve improvement in resource efficiency made possible by integrated circuit and microsystem technologies key additional considerations are packaging (area/volume) and wireless capability (energy/data).

6.1 Implantable Packaging

A key technical challenge and major constraint in developing long-term implantable medical devices (IMD) is the packaging, including connectors and any in-body leads/cables. This all needs to be biocompatible (cause no harm), biostable (not degrade), mechanically robust, compact, and provide the means to connect to the electrodes. Virtually all current clinically available IMDs use hermetically sealed titanium packages with ceramic/glass interconnect feedthroughs to a “barrel” type connector block. Implantable leads use coiled conductors (coiled to allow them to flex, stretch, compress) within polymer encapsulation. This approach, however, places a fundamental limit on the number of feedthroughs, i.e. galvanic connections into the hermetic package that are possible (due to size constraints).

If future and emerging devices are however to have 100s or 1000s of electrode connections, a different approach is needed for the packaging, and/or system architecture. One solution is to embed active electronics close to the electrodes to provide a digital interface. Therefore, connecting this to the main

module (housed in a conventional titanium package) would require fewer conductors to provide power and digital communication. This, however, transfers the challenge (from requiring more feedthroughs in the conventional package) to how to package the "active" electrodes. This can be addressed by using one of three approaches (or a combination) that include: (1) a hermetic micropackage based on metals or a crystal substrate (e.g. silicon, quartz, etc); (2) a hermetic or near-hermetic layer formed through either passivation (e.g. silicon nitride), a thin film deposition process (e.g. atomic layer deposition) or a thick film polymer coating (e.g. parylene); (3) non-hermetic polymer coating (e.g. silicone rubber) with the encapsulated circuits operating at 100% relative humidity [25]. Using such system partitioning, the core module could then connect to a few such active electrodes.

6.2 Wireless Telemetry, Power Transfer and Power Management

To achieve further upscaling in the number of channels, or the spread between these electrodes (i.e. recording and stimulation across a larger region), a recent trend, particularly in the research community (neural dust, neurograins, etc.), is to do this by distributing the neural interface across several devices (i.e. 10s, 100s or even 1000s). However, in order to do so, there is a need to be completely wireless; for both transmitting power and data communication [40]. The packaging of these wireless microsystems can use methods described previously (e.g. micropackaging), but the technical challenge then shifts to achieving an efficient distributed wireless architecture.

Wireless power transfer (WPT) and data transfer can eliminate the need for bulky batteries and wires and support significant scaling of future IMDs with extended lifetime. When considering modern implants of more than 64 electrodes, recording local field potentials and neural spikes with a sampling rate higher than 10kS/s and a resolution of at least 8 bits, power levels greater than 100 mW with data rates in excess of 5 Mbps are required [41].

Inductive coupling has been the dominant technique to support wireless powering over short distances (10-20mm) over the last decades. To comply with specific absorption rates (SAR) below 1.6 W/kg set by the U.S. Federal Communications Commission (FCC), inductive links are usually operated in the low-MHz region, including the 6.78 MHz and 13.56 MHz ISM bands [42], [43].

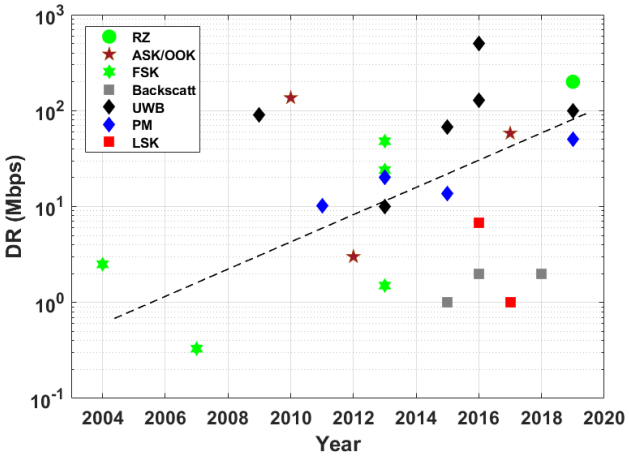


***Figure 12**. Trends in reported data rates over the last 15 years*

Carrier-less pulse-modulation (PM) schemes have recently been proposed to achieve energy-efficient high-data rates, by transmitting data using wideband pulses over inductive links. Schormans et. al recently presented a pulse-harmonic modulation (PHM) approach, coined short-range quality-factor modulation (SQuirM) that can support data rates of 50 Mbps while consuming 400 µW, resulting in an energy efficiency of 8 pJ/b [44]. The need to achieve data rates beyond 10 Mbps to accommodate high channel count in modern neural interfaces, has motivated the use of far-field (RF) links for data transfer (often in combination with inductive links for powering [45]–[47]). In far-field systems, FCC-regulated ISM bands are often used, including 433 MHz, 915 MHz and 2.4 GHz. Impulse-radio ultra-wideband (IR-UWB) communication has become increasingly popular in the domain of implantable devices, thanks to its ability to support ultra-high data rates in excess of 50 Mbps. Mirbozorgi et. al. have recently presented a UWB system working in the frequency band between 3.1 and 7 GHz, capable of achieving data rates in the order of 500 Mbps, while consuming only 3.5 mW, resulting in a high energy efficiency

of 7 pJ/bit, which is comparable to PHM in inductive links. Fig. 12 shows the trends in reported data rates achieved by different modulation schemes.

RF links will likely be the dominant choice for future high-density wireless neural implants. UWB, in particular, is poised to become the prevailing strategy to achieve energy-efficient high-data rate to support future high-density wireless neural interfaces. The demand of high data rates and moderate power levels is fuelling innovation in the field of wireless data and power transfer. Coupled with the design of ultra-low power circuits and signal processing, the design of robust and energy-efficient links will support further scaling and miniaturization of future neural implants.

7 CONCLUSIONS

This tutorial presented a general framework for bioelectronic platforms from a circuit perpective, including all of the critical components for the technology stack. In the future, the use of bioelectronic systems with complex control could usher in an era of therapies that complement pharmaceutical methods.

References

[1] N. A. Fineberg *et al.*, "The size, burden and cost of disorders of the brain in the UK," *Journal of Psychopharmacology (Oxford, England),* vol. 27, no. 9, pp. 761-770, 2013.

[2] K. Famm, B. Litt, K. J. Tracey, E. S. Boyden, and M. Slaoui, "Drug discovery: a jump-start for electroceuticals," *Nature,* vol. 496, no. 7444, pp. 159-61, Apr 11 2013.

[3] P. Khanna *et al.*, "Enabling closed-loop neurostimulation research with downloadable firmware upgrades," in *2015 IEEE Biomedical Circuits and Systems Conference (BioCAS)*, 2015, pp. 1-6.

[4] R. P. Rao, "Towards neural co-processors for the brain: combining decoding and encoding in brain-computer interfaces," *Curr Opin Neurobiol,* vol. 55, pp. 142-151, Apr 2019.

[5] S. Stanslaski *et al.*, "A Chronically-Implanted Neural Coprocessor for Exploring Treatments for Neurological Disorders," *IEEE Trans Biomed Circuits Syst,* Nov 7 2018.

[6] S. Stanslaski *et al.*, "Creating neural “co-processors” to explore treatments for neurological disorders," in *2018 IEEE International Solid - State Circuits Conference - (ISSCC)*, 2018, pp. 460-462.

[7] M. Lloyd *et al.*, "Rate adaptive pacing in an intracardiac pacemaker," *Heart Rhythm,* vol. 14, no. 2, pp. 200-205, Feb 2017.

[8] T. Denison, M. Morris, and F. Sun, "Building a bionic nervous system," *IEEE Spectrum,* vol. 52, no. 2, pp. 32-39, 2015.

[9] V. K. Rathi, N. S. Kondamuri, M. R. Naunheim, S. K. Gadkaree, R. B. Metson, and G. A. Scangas, "Use and Cost of a Hypoglossal Nerve Stimulator Device for Obstructive Sleep Apnea Between 2015 and 2018," *JAMA Otolaryngol Head Neck Surg,* Aug 22 2019.

[10] M. J. Vansteensel *et al.*, "Fully Implanted Brain-Computer Interface in a Locked-In Patient with ALS," *N Engl J Med,* vol. 375, no. 21, pp. 2060-2066, Nov 24 2016.

[11] R. Harrison, "The Design of Integrated Circuits to Observe Brain Activity," *Proceedings of the IEEE,* vol. 96, pp. 1203-1216, 08/01 2008.

[12] S. Ha *et al.*, "Silicon-Integrated High-Density Electrocortical Interfaces," *Proceedings of the IEEE,* vol. 105, no. 1, pp. 11-33, / 2017.

[13] J. J. Jun *et al.*, "Fully integrated silicon probes for high-density recording of neural activity," *Nature,* vol. 551, no. 7679, pp. 232-236, 2017/11/01 2017.

[14] N. Ahmadi *et al.*, "Towards a Distributed, Chronically-Implantable Neural Interface," in *2019 9th International IEEE/EMBS Conference on Neural Engineering (NER)*, 2019, pp. 719-724.

[15] R. M. Neely, D. K. Piech, S. R. Santacruz, M. M. Maharbiz, and J. M. Carmena, "Recent advances in neural dust: towards a neural interface platform," *Current Opinion in Neurobiology,* vol. 50, pp. 64-71, 2018/06/01/ 2018.

[16] A. Bashashati, M. Fatourechi, R. K. Ward, and G. E. Birch, "A survey of signal processing algorithms in brain-computer interfaces based on electrical brain signals," *J Neural Eng,* vol. 4, no. 2, pp. R32-57, Jun 2007.
[17] E. Noorsal, K. Sooksood, H. Xu, R. Hornig, J. Becker, and M. Ortmanns, "A neural stimulator frontend with high-voltage compliance and programmable pulse shape for epiretinal implants," *IEEE Journal of Solid-State Circuits,* Article vol. 47, no. 1, pp. 244-256, 2012, Art. no. 6025221.
[18] K. Chen, Y. K. Lo, and W. Liu, "A 37.6mm2 1024-channel high-compliance-voltage SoC for epiretinal prostheses," 2013, vol. 56, pp. 294-295.
[19] A. Urso, V. Giagka, M. Van Dongen, and W. A. Serdijn, "An Ultra High-Frequency 8-Channel Neurostimulator Circuit with 68% Peak Power Efficiency," *IEEE Transactions on Biomedical Circuits and Systems,* Article vol. 13, no. 5, pp. 882-892, 2019, Art. no. 8727437.
[20] W. Y. Hsu and A. Schmid, "Compact, Energy-Efficient High-Frequency Switched Capacitor Neural Stimulator with Active Charge Balancing," *IEEE Transactions on Biomedical Circuits and Systems,* Article vol. 11, no. 4, pp. 878-888, 2017, Art. no. 7982639.
[21] M. N. van Dongen and W. A. Serdijn, "Does a coupling capacitor enhance the charge balance during neural stimulation? An empirical study," *Med. Biol. Engineering and Computing* 54(1): 93-101 (2016)
[22] K. Sooksood, T. Stieglitz and M. Ortmanns, "An Active Approach for Charge Balancing in Functional Electrical Stimulation," in *IEEE Transactions on Biomedical Circuits and Systems*, vol. 4, no. 3, pp. 162-170, June 2010.
[23] L. Yao, P. Li, and M. Je, "A pulse-width-adaptive active charge balancing circuit with pulse-insertion based residual charge compensation and quantization for electrical stimulation applications," *2015 IEEE Asian Solid-State Circuits Conference (A-SSCC)*, Xiamen, 2015, pp. 1-4.
[24] John Hornberger, Krishna Kumar, Eric Verhulst, Mary Ann Clark and John Hernandez, "Rechargeable Spinal Cord Stimulation Versus Nonrechargeable System for Patients With Failed Back Surgery Syndrome: A Cost-Consequences Analysis," *The Clinical Journal of Pain*, vol. 24. pp. 244-52. 2008.
[25] V. Giagka and W. Serdijn, "Realizing flexible bioelectronic medicines for accessing the peripheral nerves – technology considerations," *Bioelectronic Medicine,* vol. 4, 12/01 2018.
[26] K. Deisseroth, "Optogenetics," *Nature Methods,* vol. 8, no. 1, pp. 26-29, 2011.
[27] L. Fenno, O. Yizhar, and K. Deisseroth, "The development and application of optogenetics," *Annu. Rev. Neurosci. 2011*, vol. 34, pp: 389-412, Jul. 2011.
[28] M. T. Alt, E. Fiedler, L. Rudmann, J. S. Ordonez, P. Ruther, and T. Stieglitz, "Let there be light–Optoprobes for neural implants," *Proceedings of the IEEE*, vol. 105, no. 1, pp. 101-138, Jan. 2017.
[29] J. C. Williams, and T. Denison, "From optogenetic technologies to neuromodulation therapies," *Sci. Transl. Med.,* vol. 5, no. 177, pp. 177ps6, Mar. 2013.
[30] B. Y. Chow, and E. S. Boyden, "Optogenetics and translational medicine," *Sci. Transl. Med.,* vol. 5, no. 177, pp. 177ps5, Mar. 2013.
[31] W. Legon *et al.*, "Transcranial focused ultrasound modulates the activity of primary somatosensory cortex in humans," *Nature Neuroscience,* vol. 17, no. 2, pp. 322--329, 2014.
[32] W. J. Tyler, S. W. Lani, and G. M. Hwang, "Ultrasonic modulation of neural circuit activity," *Current Opinion in Neurobiology,* vol. 50, pp. 222--231, 2018.
[33] A. Fomenko, C. Neudorfer, R. F. Dallapiazza, S. K. Kalia, and A. M. Lozano, "Low-intensity ultrasound neuromodulation: An overview of mechanisms and emerging human applications," *Brain Stimulation,* vol. 11, no. 6, pp. 1209-1217, 2018/11/01/ 2018.
[34] M. E. Downs, S. A. Lee, G. Yang, S. Kim, Q. Wang, and E. E. Konofagou, "Non-invasive peripheral nerve stimulation via focused ultrasound in vivo," *Physics in Medicine \& Biology,* vol. 63, no. 3, p. 035011, 2018.

[35] H. S. Gougheri, A. Dangi, S. Kothapalli, and M. Kiani, "A Comprehensive Study of Ultrasound Transducer Characteristics in Microscopic Ultrasound Neuromodulation," *IEEE Transactions on Biomedical Circuits and Systems,* pp. 1-1, 2019.

[36] C. Chen *et al.*, "A Front-End ASIC With Receive Sub-array Beamforming Integrated With a 32 x 32 PZT Matrix Transducer for 3-D Transesophageal Echocardiography," *IEEE Journal of Solid-State Circuits,* pp. 1--13, 2017.

[37] J. Li *et al.*, "A 1.54mW/Element 150μm-Pitch-Matched Receiver ASIC with Element-Level SAR/Shared-Single-Slope Hybrid ADCs for Miniature 3D Ultrasound Probes," in *2019 Symposium on VLSI Circuits*, 2019, pp. C220-C221.

[38] T. Costa, C. Shi, K. Tien, and K. L. Shepard, "A CMOS 2D Transmit Beamformer With Integrated PZT Ultrasound Transducers For Neuromodulation," in *2019 IEEE Custom Integrated Circuits Conference (CICC)*, 2019, pp. 1-4.

[39] E. Macé, G. Montaldo, I. Cohen, M. Baulac, M. Fink, and M. Tanter, "Functional ultrasound imaging of the brain," *Nature Methods*, vol. 8, no. 8, pp. 662-664, 2011

[40] M. Schormans, V. Valente and A. Demosthenous, "Practical Inductive Link Design for Biomedical Wireless Power Transfer: A Tutorial," *IEEE Transactions on Biomedical Circuits and Systems*, vol. 12, no. 5, pp. 1112-1130, Oct. 2018.

[41] A. Trigui, S. Hached, A. C. Ammari, Y. Savaria, and M. Sawan, “Maximizing Data Transmission Rate for Implantable Devices over a Single Inductive Link: Methodological Review,” *IEEE Rev. Biomed. Eng.*, vol. 12, pp. 72–87, 2019, doi: 10.1109/RBME.2018.2873817.

[42] D. Jiang, D. Cirmirakis, M. Schormans, T. A. Perkins, N. Donaldson, and A. Demosthenous, “An Integrated Passive Phase-Shift Keying Modulator for Biomedical Implants with Power Telemetry over a Single Inductive Link,” *IEEE Trans. Biomed. Circuits Syst.*, 2017, doi: 10.1109/TBCAS.2016.2580513.

[43] M. Kiani and M. Ghovanloo, “A 13.56-Mbps pulse delay modulation based transceiver for simultaneous near-field data and power transmission,” *IEEE Trans. Biomed. Circuits Syst.*, vol. 9, no. 1, pp. 1–11, 2015, doi: 10.1109/TBCAS.2014.2304956.

[44] M. Schormans, D. Jiang, V. Valente, and A. Demosthenous, “Short-Range Quality-Factor Modulation (SQuirM) for Low Power High Speed Inductive Data Transfer,” *IEEE Trans. Circuits Syst. I Regul. Pap.*, vol. 66, no. 9, pp. 3254–3265, Sep. 2019, doi: 10.1109/TCSI.2019.2922124.

[45] H. Kassiri *et al.*, “Battery-less Tri-band-Radio Neuro-monitor and Responsive Neurostimulator for Diagnostics and Treatment of Neurological Disorders,” *IEEE J. Solid-State Circuits*, vol. 51, no. 5, pp. 1274–1289, 2016, doi: 10.1109/JSSC.2016.2528999.

[46] S. A. Mirbozorgi, H. Bahrami, M. Sawan, L. A. Rusch, and B. Gosselin, “A Single-Chip Full-Duplex High Speed Transceiver for Multi-Site Stimulating and Recording Neural Implants,” *IEEE Trans. Biomed. Circuits Syst.*, vol. 10, no. 3, pp. 643–653, Jun. 2016, doi: 10.1109/TBCAS.2015.2466592.

[47] R. R. Harrison *et al.*, “A low-power integrated circuit for a wireless 100-electrode neural recording system,” *IEEE J. Solid-State Circuits*, vol. 42, no. 1, pp. 123–133, 2007, doi: 10.1109/JSSC.2006.886567.